Frontiers of Information Technology & Electronic Engineering
www.jzus.zju.edu.cn; engineering.cae.cn; www.springerlink.com
ISSN 2095-9184 (print); ISSN 2095-9230 (online)
E-mail: jzus@zju.edu.cn

# Supplementary materials for

Yu XUE, Xi'an FENG, 2025. Optimal federated fusion of multiple maneuvering targets based on multi-Bernoulli filters. *Front Inform Technol Electron Eng*, 26(5):753-769. https://doi.org/10.1631/FITEE.2400598

## 1 Covariance upper-bounding technique

In a network with feedback involving $S+1$ filters, let $\mathbf{P}_{sr}$ denote the cross-covariance of the $s^{\text{th}}$ and $r^{\text{th}}$ estimates, which arises from the feedback, and let $\mathbf{P}_s$ denote the self-covariance of the $s^{\text{th}}$ estimate, $\forall s, r = 0, 1, \ldots, S+1$. Expanding $\mathbf{P}_s$ to $1/\beta(s)$ times can set $\mathbf{P}_{sr}$ to zeros, as long as $\beta(s)>0$ and $\sum_{s=0}^{S}\beta(s)=1$. In the absence of correlations, i.e., $\mathbf{P}_{sr}=\mathbf{0}$, the naïve covariance convex (CC) fusion is equivalent to Bayesian optimal measurement fusion. Similarly, the correlations arising from common process noise can be eliminated by requiring each filter to expand the process noise covariance to $1/\beta(s)$ times.

## 2 Graphical summary of conditional merging

Tricolor rectangles represent the T-JMGM components described, and the dashed rectangle represents the predicted T-JMGM component that is missed by a local filter but supplemented by the master filter (Fig. S1).

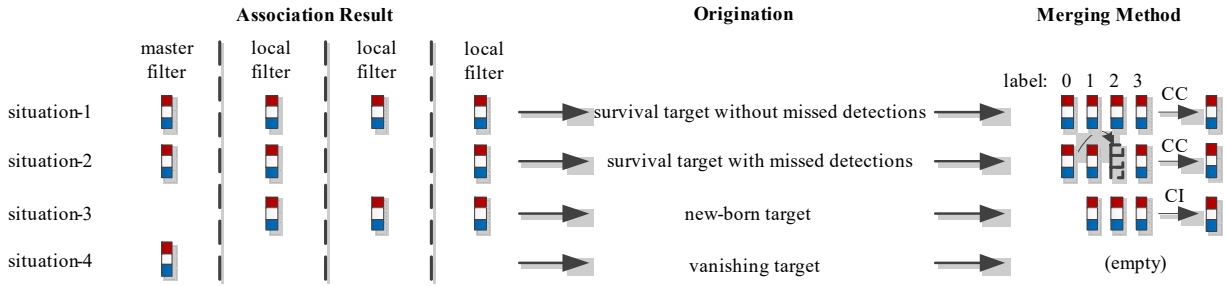


**Fig. S1 Graphical summary of conditional merging**

## 3 Sequential fusion of IMM filters and its simulation

Notice that the Bayesian fusion of IMM filters derived in our manuscript is different from the conventional sequential fusion in modifying model probabilities. The latter executes $u_m(\mathbf{z}^{(1:s)}) = L(\mathbf{z}^{(s)} \mid p_m(\mathbf{x} \mid \mathbf{z}^{(1:s-1)}))u_m(\mathbf{z}^{(1:s-1)})$, $s$=$s$+1 until $s$=$S$, where $u_m(\mathbf{z}^{(1:s-1)})$ is the probability of the $m^{\text{th}}$ model

fusing $s$–1 sensors' measurements $\mathbf{z}^{(1:s-1)}$, and $L(\mathbf{z}^{(s)} \mid p_m(\mathbf{x} \mid \mathbf{z}^{(1:s-1)}))$ is the normalized likelihood of $\mathbf{z}^{(s)}$ and state density $p_m(\mathbf{x} \mid \mathbf{z}^{(1:s-1)})$ after fusing $\mathbf{z}^{(1:s-1)}$. In the Bayesian fusion, $u_m(\mathbf{z}^{(1:S)}) = \prod_{s=1}^{S} L(\mathbf{z}^{(s)} \mid p_m(\mathbf{x}))u_m$, where $L(\mathbf{z}^{(s)} \mid p_m(\mathbf{x}))$ is the normalized likelihood of $\mathbf{z}^{(s)}$ and the prior state density $p(\mathbf{x})$ under the $m^{\text{th}}$ model. $p(\mathbf{x})$ and $p_m(\mathbf{x} \mid \mathbf{z}^{(1:s-1)})$ have been detailed in Section 3.1. In fact, the derived Bayesian fusion has been verified by Choi et al. (2024).

We simulated $S$=9 linear sensor nodes with $\mathbf{z}^{(s)} = \mathbf{H}^{(s)}\mathbf{x} + \mathbf{v}^{(s)}$, where $\mathbf{H}^{(s)} = \begin{bmatrix} 1 & 0 & 0 & 0 \\ 0 & 1 & 0 & 0 \end{bmatrix}$ is the linear observation matrix and the Gaussian observation noise $\mathbf{v}^{(s)}$ features a covariance of $\mathbf{R}^{(s)}$ =diag(25,25), $\forall s$. They cooperatively track the designed target-1.

We compared the standard IMM filter, conventional sequential fusion, and derived Bayesian fusion after 200 Monte Carlo runs. Fig. S2 illustrates the likelihood ratios of the CV and ACT models of the 1st, 3rd, 6th, and 9th sensor nodes in conventional sequential fusion. Figs. S3 and S4 present the model probability error curves (the sum of the absolute values of the differences between the model-conditioned true and estimated values) and position error curves of different algorithms, respectively.

Fig. S2 illustrates the likelihood fading issue described above: The likelihood ratio decreases as more sensors are fused. This issue reduces the ability of measurement likelihoods to modify model probabilities, so we can observe in Fig. S3 that the model probability error curve of the sequential fusion is higher than that of the Bayesian fusion. As seen in Fig. S4, the position error of the Bayesian fusion is smaller than that of the sequential fusion (by about 7.01%).

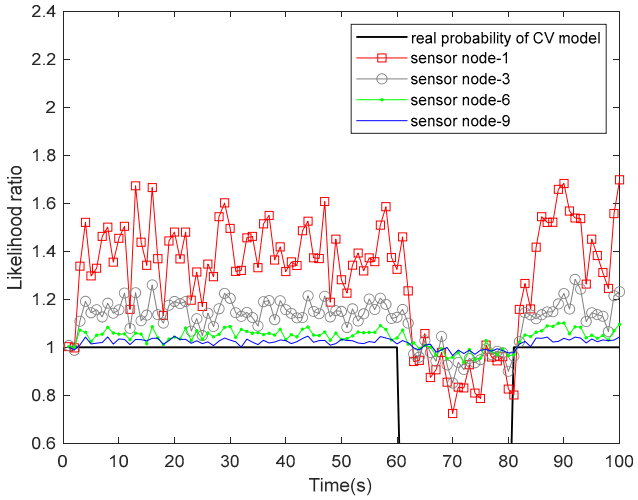


**Fig. S2 Likelihood ratios of different sensors in sequential fusion**

## 4 Centralized PM fusion of JMGM-MB filters

The PM fusion of JMGM-MB filters inherits the form of the Bayesian fusion described by Saucan et al. (2017), i.e.,

$$\pi(\mathbf{X} \mid \mathbf{Z}) \propto \prod_{s=1}^{S} p(\mathbf{Z}^{(s)} \mid \mathbf{X}) \cdot \pi(\mathbf{X}), \tag{S1}$$

where $\mathbf{X}$ is a variable of multi-target state RFS, and $\pi(\mathbf{X})$ is its prior density; $\mathbf{Z}^{(s)}$ is the measurement set of the $s^{\text{th}}$ sensor, and $p(\mathbf{Z}^{(s)} \mid \mathbf{X})$ is its likelihood function; $\pi(\mathbf{X} \mid \mathbf{Z})$ is the posterior density with $\mathbf{Z} = \bigcup_{s=1}^{S} \mathbf{Z}^{(s)}$.

Let the prior density $\pi(\mathbf{X}) = \{(r^{(v)}, p^{(v)})\}_{v=1}^{M}$, and each prior state PDF $p^{(v)} = \sum_{i=1}^{J} \omega_i^{(v)} \sum_{m=1}^{N} u_i^{(v)} \mathcal{N}(\mathbf{x}; \mathbf{m}_{i,m}^{(v)}, \mathbf{P}_{i,m}^{(v)})$. Let the fused density $\pi(\mathbf{X} \mid \mathbf{Z}) = \{(r^{(\mathrm{F},v)}, p^{(\mathrm{F},v)})\}_{v=1}^{M^{(\mathrm{F})}}$ with the $v^{\text{th}}$ fused state PDF $p^{(\mathrm{F},v)} = \sum_{i=1}^{J} \omega_i^{(\mathrm{F},v)} \sum_{m=1}^{N} u_i^{(\mathrm{F},v)} \mathcal{N}(\mathbf{x}; \mathbf{m}_{i,m}^{(\mathrm{F},v)}, \mathbf{P}_{i,m}^{(\mathrm{F},v)})$. If the $v^{\text{th}}$ fused BC $(r^{(\mathrm{F},v)}, p^{(\mathrm{F},v)})$ originates from $(r^{(v)}, p^{(v)})$ and has absorbed $\mathbf{z}^{(1)}, \mathbf{z}^{(2)}, ..., \mathbf{z}^{(S)}$ ($\mathbf{z}^{(s)} \in \mathbf{Z}^{(s)}$ and can be empty $\varnothing$), then according to the optimal Bayesian fusion, we have

$$(\mathbf{P}_{i,m}^{(\mathrm{F},v)})^{-1} \mathbf{m}_{i,m}^{(\mathrm{F},v)} = (\mathbf{P}_{i,m}^{(v)})^{-1} \mathbf{m}_{i,m}^{(v)} + \sum_{s=1}^{S} (\mathbf{H}^{(s)})^{\mathrm{T}} (\mathbf{R}^{(s)})^{-1} \mathbf{z}^{(s)}, \tag{S2}$$

$$(\mathbf{P}_{i,m}^{1:s,v})^{-1} = (\mathbf{P}_{i,m}^{(v)})^{-1} + \sum_{s=1}^{S} (\mathbf{H}^{(s)})^{\mathrm{T}} (\mathbf{R}^{(s)})^{-1} \mathbf{H}^{(s)}, \tag{S3}$$

$$u_{i,m}^{(\mathrm{F},v)} = \frac{\prod_{s=1}^{S} g_m(\mathbf{z}^{(s)}) \cdot u_{i,m}^{(v)}}{\sum_{m=1}^{N} \prod_{s=1}^{S} g_m(\mathbf{z}^{(s)}) \cdot u_{i,m}^{(v)}}, \tag{S4}$$

where $g_m(\mathbf{z}^{(s)}) = \int g(\mathbf{z}^{(s)} \mid \mathbf{x}, m) \mathcal{N}(\mathbf{x}; \mathbf{m}_{i,m}^{(v)}, \mathbf{P}_{i,m}^{(v)}) \mathrm{d}\mathbf{x}$ and $g_m(\varnothing) = 1$.

To compute $g_m(\mathbf{z}^{(s)})$, each JMGM component is required to always remember the estimates and error covariances of its ancestor $(\mathbf{m}_{i,m}^{(v)}, \mathbf{P}_{i,m}^{(v)})_{m=1}^{N}$ originating from the prediction or target new birth. After fusing the measurements of all sensors, pruning and merging operations are necessary to limit computation volume. The propagation of other parameters, including weights $\omega$ and existence probabilities $r$, is the same as for the standard JMGM-MB filter.

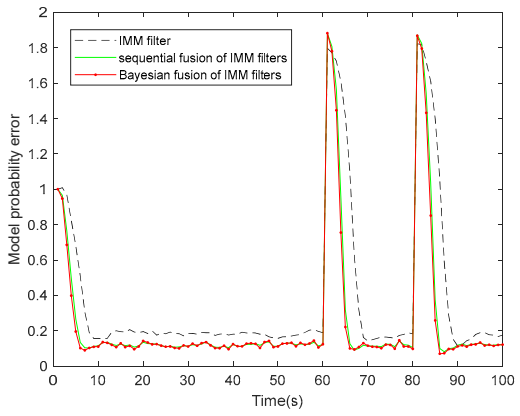


**Fig. S3 Single-target model probability error curves of different algorithms**

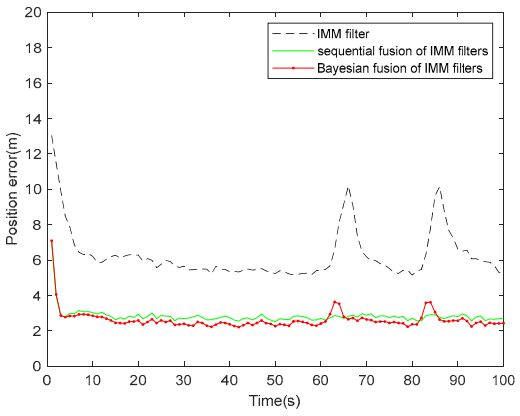


**Fig. S4 Single-target position error curves of different algorithms**

## 5 Decentralized AA fusion of JMGM-MB filters

The AA fusion is similar to the proposed federated fusion except that no master filter is involved, and the JMGM components are merged using the same method.

Assume that the multi-target density of the $s^{\text{th}}$ sensor node at time $k$ is $\pi_k^{(s)} = \{(r_k^{(s,v)}, p_k^{(s,v)})\}_{v=1}^{M_k^{(s)}}$ with $p_k^{(s,v)} = \sum_{i=1}^{J_k^{(s,v)}} \omega_{k,i}^{(s,v)} \sum_{m=1}^{N} u_{k,i,m}^{(s,v)} \mathcal{N}(\mathbf{x}; \mathbf{m}_{k,i,m}^{(s,v)}, \mathbf{P}_{k,i,m}^{(s,v)})$, $s$=1, 2, …, $S$. Each sensor node extracts its round$(\sum_{v=1}^{M_k^{(s)}} r_k^{(s,v)})$ T-BCs. When receiving these T-BCs, the fusion node weights them with positive sensor

weights $\alpha(s)$, $\sum_{s=1}^{S}\alpha(s)=1$. Then, all T-BCs are uniformly recorded as $\{(r_{\mathrm{T},k}^{(v)}, p_{\mathrm{T},k}^{(v)})\}_{v=1}^{\sum_{s=1}^{S}\hat{N}_k^{(s)}}$. The T-BCs that satisfy $(\tilde{\mathbf{x}}_k^{(vu)})^{\mathrm{T}}(\mathbf{P}_k^{(v)}+\mathbf{P}_k^{(u)})^{-1}\tilde{\mathbf{x}}_k^{(vu)}<\lambda_{\mathrm{m}}$ will be merged into one, where $\hat{\mathbf{x}}_k^{(v)}$ and $\mathbf{P}_k^{(v)}$ represent the estimate and error covariance of the $v^{\mathrm{th}}$ T-BC, respectively; the estimate residual $\tilde{\mathbf{x}}_k^{(vu)}=\hat{\mathbf{x}}_k^{(v)}-\hat{\mathbf{x}}_k^{(u)}$. Of course, the JMGM components with distances that are too small will be merged into one. After association and merging, BCs with existence probabilities smaller than $\lambda_{\mathrm{d}}^{\mathrm{BC}}$ and JMGM components with weights smaller than $\lambda_{\mathrm{d}}^{\mathrm{JMGM}}$ will be discarded.

## References

Choi J, Park J, Huh K, 2024. Robust object tracking against sensor failures with centralized IMM filter. *IEEE Access*, 12:85203-85218. https://doi.org/10.1109/ACCESS.2024.3415381

Saucan AA, Coates MJ, Rabbat M, 2017. A multisensor multi-Bernoulli filter. *IEEE Trans Signal Process*, 65(20):5495-5509. https://doi.org/10.1109/TSP.2017.2723348